Peak Filter Tuning based on Disturbance Spectrum for MIMO High-Precision Scan Stage

Masahiro Mae * **Wataru Ohnishi** * **Hiroshi Fujimoto** *
Koichi Sakata ** **Atsushi Hara** **

* *The University of Tokyo, 5-1-5, Kashiwanoha, Kashiwa, Chiba, 277-8561, Japan (e-mail: mmae@ieee.org, ohnishi@ieee.org, fujimoto@k.u-tokyo.ac.jp)*
** *Nikon Corporation, 47-1, Nagaodaicho, Sakae, Yokohama, Kanagawa, 244-8533, Japan (e-mail: koichi.sakata@nikon.com, atsushi.hara@nikon.com)*

Abstract: In high-precision positioning systems such as scanning machines, the feedback controller tuning needs a lot of time and skills. In particular, a feedback controller tuning with six-degree-of-freedoms $(x, y, \theta_z, z, \theta_x, \theta_y)$ is difficult because of the numbers of controller parameters in each axis. The feedback controllers designed as single-input single-output controllers in each axis may not achieve sufficient performance in multi-input multi-output systems, and stability may not be satisfied because of a coupling problem between each axis. The repetitive disturbance makes the performance worse in a constant velocity scanning motion, and they are conventionally rejected by a peak filter in other applications of high-precision systems such as a hard disk drive. In this paper, we propose a tuning method of a peak filter to suppress a repetitive disturbance which satisfies robust stability conditions for six-degree-of-freedom systems by using convex optimization. The effectiveness of the proposed method is verified by the error in the constant velocity scanning motion.

Keywords: Concave-convex procedure, Data based tuning, Frequency responses, Disturbance rejection, Peak filter, Feedback control, MIMO system

1. INTRODUCTION

In high-precision motion control systems in industries, the cost of tuning controllers becomes very large due to mass productions and demands of a factory automation. In particular, the high-precision scanning systems such as manufacturing semiconductors and liquid crystal panels need much cost of tuning controllers because of the necessity of achieving very small tracking errors and growing needs of PCs and smartphones.

In these applications, the high-precision stages have 6 degrees of freedoms (6-DOFs) $(x, y, \theta_z, z, \theta_x, \theta_y)$ to achieve high-precision tracking performance [Butler (2011); Oomen (2018); Mae et al. (2019)]. Therefore, these stages become multi-input multi-output (MIMO) systems, and the number of controller parameters in each axis becomes enormous. MIMO systems are difficult to model due to a coupling problem between each axis and modeling errors occur frequently. Therefore, it is desirable to tune the controller from not the model but the frequency response data obtained by the experiment directly. Several optimization methods for tuning controller parameters from frequency response data are proposed, such as genetic algorithm [Tang et al. (2001)], Nelder-Mead method [Lee et al. (1985)], particle swarm optimization [Gaing (2004)]. Especially, the methods based on convex optimization are proposed such as loop shaping method [Karimi and Galdos (2010)], bundle method [Do and Artieres (2012); Kitayoshi and Fujimoto (2019)], and sequential linearization method [Hast et al. (2013); Shinoda et al. (2017); Ohnishi (2019)] using Concave-Convex Procedure (CCCP) [Yuille and Rangarajan (2003)]. Concave-Convex Procedure has a characteristic that the solution will converge to a saddle point or a local minimum. Even though, when we design controllers of MIMO systems, Concave-Convex Procedure is preferable because MIMO systems are difficult to model and this method can be used to the frequency response data, directly.

In these high-precision scan stages, disturbances due to the motor cogging and the vibration from the ground deteriorate the tracking performance. These disturbances should be suppressed by feedback control. Several disturbances such as the cogging of the motor have repetitive characteristics. Previous studies show that repetitive disturbances are effectively suppressed by using a peak filter with the same frequency as the repetitive disturbance frequency, mainly in the hard disk drive field [Atsumi et al. (2007)]. On the other hand, multi-axis high-precision scan stages have a risk to become unstable because a coupling problem between each axis occur due to other axis controllers that are high gained by peak filter. Therefore, peak filters have not been used for multi-axis high-precision stages so far.

From these backgrounds, this paper proposes an auto-tuning method of a peak filter in order to suppress repetitive disturbance of multi-axis high-precision scan stages which satisfies robust stability conditions including a coupling problem between each axis of MIMO systems by using convex optimization.

2. STRUCTURE OF CONTROLLED SYSTEM

2.1 Details of plant

We think about a 6-input 6-output high-precision scan stage with 6-DOFs $(x, y, \theta_z, z, \theta_x, \theta_y)$. We consider suppressing repetitive disturbance by using peak filters in a constant velocity region such as a scan motion. In this paper, we mainly handle the translation along the x axis which is the main stroke of the stage.

2.2 Details of controller

The block diagram of the controlled system is shown in Fig. 1. The block $\boldsymbol{P}$, $\boldsymbol{F}$ and $\boldsymbol{C}$ denote a plant, a peak filter, and given fixed controllers respectively. In order to simplify the controller structure, $\boldsymbol{F}$ and $\boldsymbol{C}$ are designed only for diagonal terms. Details of the controller structure are shown in Fig. 2. The given fixed controllers $\boldsymbol{C}$ consist of PID controllers, disturbance observers, phase lead filters, and notch filters. In this paper, the parameters of $\boldsymbol{C}$ are fixed, and the peak filter $\boldsymbol{F}$ is designed to be added to the original controlled system.

2.3 Repetitive disturbance rejection using peak filter

In high-precision positioning systems such as a hard disk drive, a repetitive disturbance d shown in Fig. 3 is suppressed by the peak filter F_{Peak} which has the same frequency to the repetitive disturbance frequency according to the internal model principle [Atsumi et al. (2007)]. In this paper, we design a peak filter to suppress repetitive disturbances for a multi-axis high-precision scan stages in which a peak filter has not been used because the MIMO systems whose gain becomes high by the peak filter may be unstable due to a coupling problem between each axis.

The peak filter designed in this paper is shown in (1).

$$F_{\mathrm{Peak}}(\mathrm{j}\omega, \rho, \eta) = \frac{s^2 + 2\rho\omega s + \omega^2}{s^2 + 2\eta\omega s + \omega^2} = \frac{F_n(\mathrm{j}\omega, \rho)}{F_d(\mathrm{j}\omega, \eta)} \quad (0 \le \eta < \rho \le 1) \tag{1}$$

ω is the resonant frequency of the peak filter. ρ and η are the damping coefficients, and ρ must be larger than η. It is noted that when ρ is smaller than η it becomes a notch filter.

3. AUTO TUNING METHOD OF PEAK FILTER USING CONVEX OPTIMIZATION

In order to evaluate robust stability conditions for the frequency response data of the system, Nyquist diagram is used. In this paper, the gain and phase margins are treated as a circle condition and coupling effects are evaluated by using generalized Gershgorin bands on the Nyquist diagram for each axis, as shown in Fig. 4.

3.1 Robust controller design with circle condition of gain mergin and phase margin

The center $(-\sigma, 0\mathrm{j})$ and radius r_m of a circle condition on the Nyquist diagram can be calculated from the gain margin g_m and the phase margin Φ_m, as shown in (2) and (3) [Maeda and Iwasaki (2014)].

$$\sigma = \frac{g_m^2 - 1}{2g_m(g_m \cos\Phi_m - 1)} \tag{2}$$

$$r_m = \frac{(g_m - 1)^2 + 2g_m(1 - \cos\Phi_m)}{2g_m(g_m \cos\Phi_m - 1)} \tag{3}$$

When the controller is stable and the open-loop frequency response does not cross the circle condition on the Nyquist diagram, the controller satisfies robust stability conditions for the gain margin g_m and the phase margin Φ_m.

3.2 Robust controller design with generalized Gershgorin bands for MIMO system

The feedback controller may become unstable due to a coupling problem between each axis even when the controller satisfies the stability condition for each axis. In this paper, we evaluate the coupling effect in the open-loop frequency response of MIMO systems by using generalized Gershgorin bands [Rosenbrock (1969); Araki and Nwokah (1975); Sebe (1996)].

$\boldsymbol{P}$, $\boldsymbol{C}$, and $\boldsymbol{F}$ which denote a plant, a peak filter, and given fixed controllers are defined as (4), (5), and (6), respectively. The parameters of peak filter $\boldsymbol{\rho}$ and $\boldsymbol{\eta}$ are also defined as (7) and (8), respectively.

$$\boldsymbol{P}(\mathrm{j}\omega_k) = P_{ij}(\mathrm{j}\omega_k) \quad (i, j = 1, 2, \ldots, n) \tag{4}$$

$$\boldsymbol{C}(\mathrm{j}\omega_k) = \begin{cases} C_i(\mathrm{j}\omega_k) & (i = j) \\ 0 & (i \neq j) \end{cases} \quad (i, j = 1, 2, \ldots, n) \tag{5}$$

$$\boldsymbol{F}(\mathrm{j}\omega_k, \boldsymbol{\rho}, \boldsymbol{\eta}) = \begin{cases} \frac{F_{n_i}(\mathrm{j}\omega_k, \rho_i)}{F_{d_i}(\mathrm{j}\omega_k, \eta_i)} & (i = j) \\ 0 & (i \neq j) \end{cases} \quad (i, j = 1, 2, \ldots, n) \tag{6}$$

$$\boldsymbol{\rho} = [\rho_1 \ \rho_2 \ \cdots \ \rho_n]^{\mathsf{T}} \tag{7}$$

$$\boldsymbol{\eta} = [\eta_1 \ \eta_2 \ \cdots \ \eta_n]^{\mathsf{T}} \tag{8}$$

It is noted that the numbers of inputs and outputs of the plant are both n in this paper.

The interaction index λ of the plant $\boldsymbol{P}$ is calculated in (9) as the maximum eigenvalue of the matrix $\boldsymbol{M}$ which is defined as (10).

$$\lambda(\mathrm{j}\omega_k) = \max(|\mathrm{eig}(\mathrm{j}\omega_k|\boldsymbol{M})|) \tag{9}$$

$$\boldsymbol{M}(\mathrm{j}\omega_k) = \begin{cases} 0 & (i = j) \\ \left|\frac{P_{ij}(\mathrm{j}\omega_k)}{P_{jj}(\mathrm{j}\omega_k)}\right| & (i \neq j) \end{cases} \quad (i, j = 1, 2, \ldots, n) \tag{10}$$

The open-loop frequency response data at each frequency on the Nyquist diagram of each axis can move within the radius r_{g_i} which is defined as (11) when MIMO plants have a coupling problem between each axis.

$$r_{g_i}(\mathrm{j}\omega_k) = \lambda(\mathrm{j}\omega_k) \left| \frac{P_{ii}(\mathrm{j}\omega_k) F_{n_i}(\mathrm{j}\omega_k, \rho) C_i(\mathrm{j}\omega_k)}{F_{d_i}(\mathrm{j}\omega_k, \eta)} \right| \quad (i, j = 1, 2, \ldots, n) \tag{11}$$

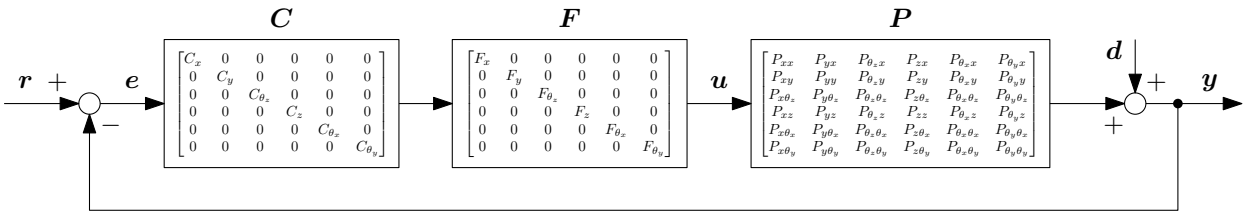

Fig. 1. Block diagram of 6-DOF controlled system.

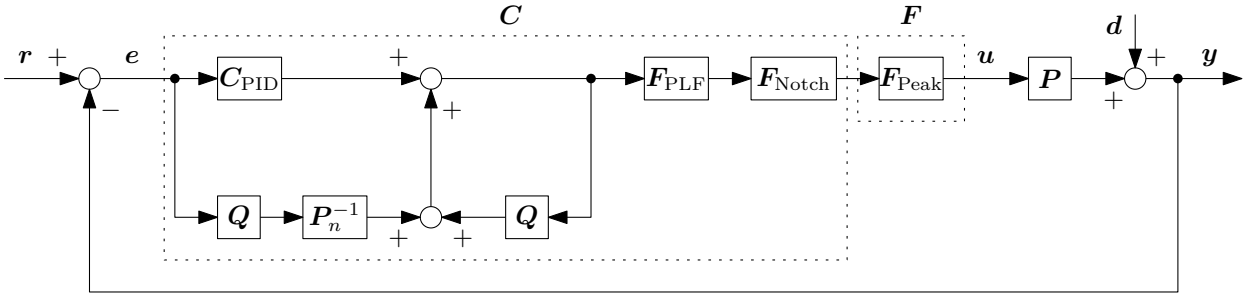

Fig. 2. Block diagram of detail in each controller.

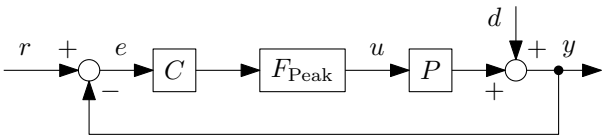

Fig. 3. Block diagram of controlled system with peak filter.

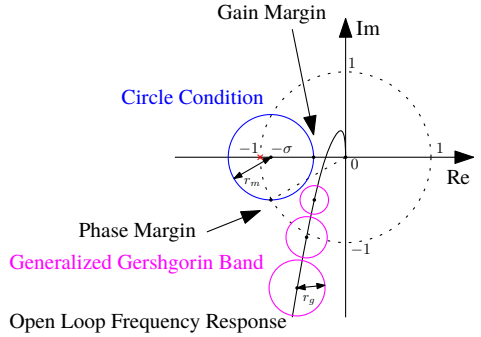

Fig. 4. Circle condition of gain margin, phase margin and generalized Gershgorin bands.

The multiple circles in which the open-loop frequency response data can move are called as generalized Gershgorin bands. When the controller is stable and generalized Gershgorin bands do not include the point of $(-1, 0\mathrm{j})$ on the Nyquist diagram, the system satisfies a stability condition for MIMO systems with a coupling problem between each axis.

3.3 Design of weighting function of sensitivity function

The sensitivity function $\boldsymbol{S}$, defined as (12), should be small in the main frequency range of the disturbance because it is the transfer function from disturbance $\boldsymbol{d}$, defined as (13), to error $\boldsymbol{e}$, defined as (14), in Fig. 1.

$$\begin{aligned}\boldsymbol{S}(\mathrm{j}\omega_k) &= (\boldsymbol{I} + \boldsymbol{P}(\mathrm{j}\omega_k)\boldsymbol{C}(\mathrm{j}\omega_k))^{-1} \\ &= S_{ij}(\mathrm{j}\omega_k) \quad (i,j = 1,2,\ldots,n) \end{aligned} \tag{12}$$

$$\boldsymbol{d}(\mathrm{j}\omega_k) = [d_1(\mathrm{j}\omega_k)\ d_2(\mathrm{j}\omega_k)\ \cdots\ d_n(\mathrm{j}\omega_k)]^{\mathsf{T}} \tag{13}$$

$$\boldsymbol{e}(\mathrm{j}\omega_k) = [e_1(\mathrm{j}\omega_k)\ e_2(\mathrm{j}\omega_k)\ \cdots\ e_n(\mathrm{j}\omega_k)]^{\mathsf{T}} \tag{14}$$

In this paper, the frequency spectrum of the disturbance in the constant velocity region is calculated from the frequency spectrum of the error by the inverse of the sensitivity function, as shown in (15).

$$\boldsymbol{d}(\mathrm{j}\omega_k) = \boldsymbol{S}^{-1}(\mathrm{j}\omega_k)\boldsymbol{e}(\mathrm{j}\omega_k) \tag{15}$$

Then, the weighting functions of the sensitivity function $\boldsymbol{W}_S$, defined as (16), is designed by adjusting the frequency spectrum of the disturbance by the scaling parameter α_i as shown in (17) [Atsumi and Messner (2012)].

$$\boldsymbol{W}_S(\mathrm{j}\omega_k) = [W_{S_1}(\mathrm{j}\omega_k)\ W_{S_2}(\mathrm{j}\omega_k)\ \cdots\ W_{S_n}(\mathrm{j}\omega_k)]^{\mathsf{T}} \tag{16}$$

$$|W_{S_i}(\mathrm{j}\omega_k)| = \alpha_i |d_i(\mathrm{j}\omega_k)| \quad (i = 1,2,\ldots,n) \tag{17}$$

We design the controller so that the sensitivity function S satisfies the robust stability condition (18) for the weighting function of the sensitivity function W_S for each axis.

$$|S_{ii}(\mathrm{j}\omega_k)W_{S_i}(\mathrm{j}\omega_k)| \leq 1 \quad (i = 1,2,\ldots,n) \tag{18}$$

The weighting function of the sensitivity function W_S are designed from the frequency spectrum of the disturbance. The controller is tuned so that the sensitivity function satisfies a robust stability condition for larger scaling parameters α_i.

3.4 Optimization problem formulation

From the considerations above, the optimization problem of designing a peak filter which satisfies robust stability conditions for MIMO systems can be described from (19) to (23).

$$\underset{\rho_i,\eta_i}{\text{maximize}} \quad \alpha_i \quad (i=1,2,\ldots,n) \tag{19}$$

$$\text{subject to} \quad \overset{\forall}{k}$$

$$r_m - \left| \frac{P_{ii}(\mathrm{j}\omega_k)C_i(\mathrm{j}\omega_k)F_{n_i}(\mathrm{j}\omega_k,\rho_i)}{F_{d_i}(\mathrm{j}\omega_k,\eta_i)} + \sigma \right| \leq 0 \tag{20}$$

$$r_{g_i}(\mathrm{j}\omega_k) - \left| \frac{P_{ii}(\mathrm{j}\omega_k)C_i(\mathrm{j}\omega_k)F_{n_i}(\mathrm{j}\omega_k,\rho_i)}{F_{d_i}(\mathrm{j}\omega_k,\eta_i)} + 1 \right| \leq 0 \tag{21}$$

$$|W_{S_i}(\mathrm{j}\omega_k)| - \left| \frac{P_{ii}(\mathrm{j}\omega_k)C_i(\mathrm{j}\omega_k)F_{n_i}(\mathrm{j}\omega_k,\rho_i)}{F_{d_i}(\mathrm{j}\omega_k,\eta_i)} + 1 \right| \leq 0 \tag{22}$$

$$0 \leq \eta_i \leq \eta_i^{\max} < \rho_i^{\min} \leq \rho_i \leq 1 \tag{23}$$

3.5 Concave-Convex Procedure (CCCP)

The constraints of (20), (21), and (22) are concave functions because they are the difference of the convex functions, respectively. Therefore, they are not solved as convex optimization. In addition, it is also the problem that the peak filter has tuning parameters not only in the numerator but also in the denominator. In this paper, we use a sequential linearization method by using Concave-Convex Procedure with tuning parameters in the numerator and the denominator is used to transform from the concave optimization problem into the convex optimization problem [Nakamura et al. (2017)].

First, we consider a constraint of the circle condition (20). We multiply the denominator $|F_d(\mathrm{j}\omega_k,\eta)|$ on both sides of (20), and we get (24). Second, we consider a first-order approximation of the difference term in (24), and we get the convex optimization problem (25).

The same procedure is applied to a constraint of the robust stability condition for MIMO systems (21) and a constraint of sensitivity functions (22). First, we multiply the denominator $|F_d(\mathrm{j}\omega_k,\eta)|$ on both sides of (21) and (22), and we get (26) and (28), respectively. Second, we consider a first-order approximation of the difference term in (26) and (28), and we get the convex optimization problem (27) and (29), respectively.

By using the sequential linearization method, it is possible to transform from a concave optimization problem into a convex optimization problem. It is noted that $\rho_{i_{l-1}}$ and $\eta_{i_{l-1}}$ are the parameters of the optimization results in the previous iteration, and this optimization problem can be solved as a convex optimization problem by iterative calculations. In this paper, we use a dichotomy method as an iterative algorithm.

4. SIMULATION EVALUATION

The controllers can be designed independently at each axis for MIMO systems by using the proposed method. In this paper, we consider tuning a peak filter to reject a repetitive disturbance in the translation along the x axis which is the main stroke of the stage.

4.1 Condition of optimization

The number of the frequency response data of the plant is 1000. The data are arranged at logarithmically even intervals in the range of 1 Hz to 500 Hz. In the robust stability condition for MIMO system (21), we consider generalized Gershgorin bands only in the frequency range $f_c/2 \leq f < 2f_c$, when f_c is the gain cross over frequency of the open-loop transfer function without using the peak filter and the stability condition is most affected in this frequency range, so that the controllers should not be designed too conservative. In other frequencies, the interference index set to $\lambda(\mathrm{j}\omega_k) = 0$. The gain margin and the phase margin are set to 4 dB and 20 deg, respectively. This condition is satisfied in the controller without a peak filter.

The number of designed peak filters is one, and the resonant frequency ω of the peak filter is set to a constant frequency in which the power spectra of the error at each axis is the maximum. In this paper, we design the peak filter only in the translation along the x axis which is the main stroke of the stage, and the peak filters in other DOFs are set to 1. The resonant frequency ω_x of the peak filter in the translation along the x axis is set to $\omega_x = 44.9\,\mathrm{rad/s}$ ($f_x = 6.67\,\mathrm{Hz}$). The parameters of the given fixed controllers $\boldsymbol{C}$ are fixed. From the difference of the error spectrum at the peak and the low frequency, the gain of peak filter should be larger than $60\,\mathrm{dB} = 10^3$. Therefore, the parameter constraints of the peak filter (23) is set to the range in $\rho_x^{\min} = 1\times10^{-6}$ and $\eta_x^{\max} = 1\times10^{-9}$, and the initial value of each parameter is set to $\rho_x^{\mathrm{ini}} = 1\times10^{-6}$ and $\eta_x^{\mathrm{ini}} = 0$, respectively. A Nyquist diagram using the initial peak filter is shown in Fig. 5.

The dichotomy method is used to solve the convex optimization problem sequentially linearized by using Concave-Convex Procedure in the range of $\alpha_x^{\min} \leq \alpha_x \leq \alpha_x^{\max}$. The range of α_x is set to $\alpha_x^{\min} = 1\times10^5$ and $\alpha_x^{\max} = 1\times10^7$. The sensitivity function and the weighting fuction of the sensitivity function are shown in Fig. 6. The iterative optimization by the dichotomy method is repeated until $\frac{\alpha_x^{\mathrm{ng}}}{\alpha_x^{\mathrm{ok}}} \times 100 = 1\,\%$, when α_x^{ok} and α_x^{ng} are defined as the value of α_x in the feasible and infeasible solutions, respectively. The optimization problem is calculated by using YALMIP [Lofberg (2004)] and Mosek [MosekApS (2019)].

4.2 Peak filter design

The parameters of the optimal peak filter and the evaluation function are designed as $\rho_x^{\mathrm{opt}} = 0.0065$, $\eta_x^{\mathrm{opt}} = 0$, and $\alpha_x^{\mathrm{opt}} = 941113$, respectively.

The Nyquist diagram with the optimal peak filter is shown in Fig. 7. It is confirmed that the designed controller satisfies the robust stability conditions.

The sensitivity function and the weighting function of the sensitivity function with the optimal peak filter are shown in Fig. 8. It is confirmed that the controller gain at the frequency with the maximum disturbance spectrum becomes high due to using the peak filter, and the gain of the sensitivity function becomes low.

4.3 Evaluation of repetitive disturbance rejection

The performance of the high-precision scan stage in a constant velocity scanning motion is evaluated by the difference between the maximum value and the minimum value of the error. The error with the peak filter $\boldsymbol{e}^{\mathrm{opt}}$ is

$$r_m|F_{d_i}(\mathrm{j}\omega_k,\eta_i)| - |P_{ii}(\mathrm{j}\omega_k)C_i(\mathrm{j}\omega_k)F_{n_i}(\mathrm{j}\omega_k,\rho_i) + \sigma F_{d_i}(\mathrm{j}\omega_k,\eta_i)| \le 0 \quad (i=1,2,\ldots,n) \tag{24}$$

$$\begin{aligned} &r_m|F_{d_i}(\mathrm{j}\omega_k,\eta_{i_l})| \\ &- \mathrm{Re}\left(\frac{(P_{ii}(\mathrm{j}\omega_k)C_i(\mathrm{j}\omega_k)F_{n_i}(\mathrm{j}\omega_k,\rho_{i_{l-1}}) + \sigma F_{d_i}(\mathrm{j}\omega_k,\eta_{i_{l-1}}))^*}{|P_{ii}(\mathrm{j}\omega_k)C_i(\mathrm{j}\omega_k)F_{n_i}(\mathrm{j}\omega_k,\rho_{i_{l-1}}) + \sigma F_{d_i}(\mathrm{j}\omega_k,\eta_{i_{l-1}})|}(P_{ii}(\mathrm{j}\omega_k)C_i(\mathrm{j}\omega_k)F_{n_i}(\mathrm{j}\omega_k,\rho_{i_l}) + \sigma F_{d_i}(\mathrm{j}\omega_k,\eta_{i_l}))\right) \le 0 \\ &(i=1,2,\ldots,n) \end{aligned} \tag{25}$$

$$r_{g_i}(\mathrm{j}\omega_k)|F_{d_i}(\mathrm{j}\omega_k,\eta_i)| - |P_{ii}(\mathrm{j}\omega_k)C_i(\mathrm{j}\omega_k)F_{n_i}(\mathrm{j}\omega_k,\rho_i) + F_{d_i}(\mathrm{j}\omega_k,\eta_i)| \le 0 \quad (i=1,2,\ldots,n) \tag{26}$$

$$\begin{aligned} &r_{g_i}(\mathrm{j}\omega_k)|F_{d_i}(\mathrm{j}\omega_k,\eta_i)| \\ &- \mathrm{Re}\left(\frac{(P_{ii}(\mathrm{j}\omega_k)C_i(\mathrm{j}\omega_k)F_{n_i}(\mathrm{j}\omega_k,\rho_{i_{l-1}}) + F_{d_i}(\mathrm{j}\omega_k,\eta_{i_{l-1}}))^*}{|P_{ii}(\mathrm{j}\omega_k)C_i(\mathrm{j}\omega_k)F_{n_i}(\mathrm{j}\omega_k,\rho_{i_{l-1}}) + F_{d_i}(\mathrm{j}\omega_k,\eta_{i_{l-1}})|}(P_{ii}(\mathrm{j}\omega_k)C_i(\mathrm{j}\omega_k)F_{n_i}(\mathrm{j}\omega_k,\rho_{i_l}) + F_{d_i}(\mathrm{j}\omega_k,\eta_{i_l}))\right) \le 0 \\ &(i=1,2,\ldots,n) \end{aligned} \tag{27}$$

$$|W_{S_i}(\mathrm{j}\omega_k)F_{d_i}(\mathrm{j}\omega_k,\eta_i)| - |P_{ii}(\mathrm{j}\omega_k)F_{n_i}(\mathrm{j}\omega_k,\rho_i)C_i(\mathrm{j}\omega_k) + F_{d_i}(\mathrm{j}\omega_k,\eta_i)| \le 0 \quad (i=1,2,\ldots,n) \tag{28}$$

$$\begin{aligned} &|W_{S_i}(\mathrm{j}\omega_k)F_{d_i}(\mathrm{j}\omega_k,\eta_i)| \\ &- \mathrm{Re}\left(\frac{(P_{ii}(\mathrm{j}\omega_k)F_{n_i}(\mathrm{j}\omega_k,\rho_{i_{l-1}})C_i(\mathrm{j}\omega_k) + F_{d_i}(\mathrm{j}\omega_k,\eta_{i_{l-1}}))^*}{|P_{ii}(\mathrm{j}\omega_k)F_{n_i}(\mathrm{j}\omega_k,\rho_{i_{l-1}})C_i(\mathrm{j}\omega_k) + F_{d_i}(\mathrm{j}\omega_k,\eta_{i_{l-1}})|}(P_{ii}(\mathrm{j}\omega_k)F_{n_i}(\mathrm{j}\omega_k,\rho_{i_l})C_i(\mathrm{j}\omega_k) + F_{d_i}(\mathrm{j}\omega_k,\eta_{i_l}))\right) \le 0 \\ &(i=1,2,\ldots,n) \end{aligned} \tag{29}$$

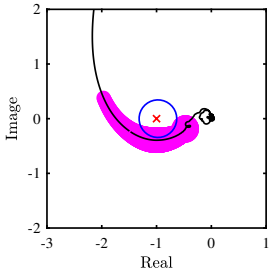

Fig. 5. Nyquist diagram of initial condition in translation along x axis.

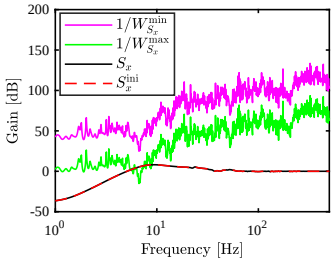

Fig. 6. Sensitivity function and weighting function of initial condition in translation along x axis.

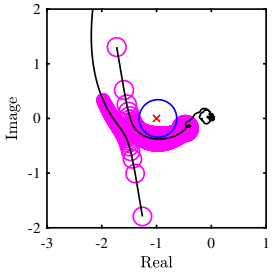

Fig. 7. Nyquist diagram of optimal condition in translation along x axis.

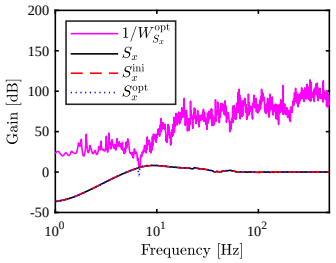

Fig. 8. Sensitivity function and weighting function of optimal condition in translation along x axis.

calculated from the error without the peak filter $\boldsymbol{e}$, as shown in (30).

$$\begin{aligned} \boldsymbol{e}^{\mathrm{opt}}(\mathrm{j}\omega_k) =& \boldsymbol{S}^{\mathrm{opt}}(\mathrm{j}\omega_k)\boldsymbol{S}^{-1}(\mathrm{j}\omega_k)\boldsymbol{e}(\mathrm{j}\omega_k) \\ =& (\boldsymbol{I} + \boldsymbol{P}(\mathrm{j}\omega_k)\boldsymbol{F}(\mathrm{j}\omega_k,\boldsymbol{\rho},\boldsymbol{\eta})\boldsymbol{C}(\mathrm{j}\omega_k))^{-1} \\ & (\boldsymbol{I} + \boldsymbol{P}(\mathrm{j}\omega_k)\boldsymbol{C}(\mathrm{j}\omega_k))\boldsymbol{e}(\mathrm{j}\omega_k) \end{aligned} \tag{30}$$

A comparison of the error without and with the peak filter in the translation along the x axis in a constant velocity region is shown in Fig. 9. It is confirmed that the difference between the maximum and minimum errors is reduced.

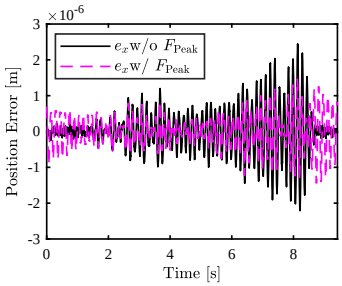

Fig. 9. Position error e_x in translation along x axis without and with peak filter in constant velocity region.

A comparison of the power spectra of the error without and with the peak filter in the translation along the x axis in a constant velocity region is shown in Fig. 10. It is confirmed that the error around 6.67 Hz which is the peak frequency of the error power spectra is reduced.

The difference between the maximum and minimum errors in 6-DOFs $(x, y, \theta_z, z, \theta_x, \theta_y)$ are shown in Table 1. The difference between the maximum and minimum error in the translation along the x axis is reduced about 37 %, while those of other DOFs are changed about 1 %. It is confirmed that the error in the translation along the x axis can be reduced without affecting other DOFs. From the evaluation above, the effectiveness of the proposed method is verified.

5. CONCLUSION

In this paper, we proposed a method of tuning a peak filter automatically to reject repetitive disturbances by using convex optimization for a multi-axis high-precision scan stage in a constant velocity scanning motions. By using the circle condition of the gain margin and the phase margin and generalized Gershgorin bands of the MIMO system, a designed controller satisfied robust stability conditions for a multi-input multi-output system with a coupling problem between each axis. In addition, the weighting function of the sensitivity function is designed from the

Table 1. Peak to peak error without and with peak filter in constant velocity region.

Axis	e_x [m]	e_y [m]	e_{θ_z} [rad]	e_z [m]	e_{θ_x} [rad]	e_{θ_y} [rad]
w/o F_{Peak}	4.65×10^{-6}	8.74×10^{-7}	8.48×10^{-7}	6.85×10^{-6}	1.16×10^{-6}	1.06×10^{-5}
w/ F_{Peak}	2.92×10^{-6}	8.85×10^{-7}	8.48×10^{-7}	6.86×10^{-6}	1.15×10^{-6}	1.06×10^{-5}

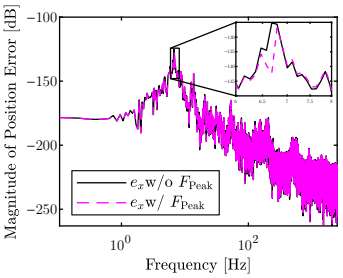

Fig. 10. Power spectra of position error e_x in translation along x axis without and with peak filter in constant velocity region.

disturbance spectrum calculated from the error spectrum so that the actual characteristic of the disturbance is considered. The concave optimization problem is transformed into the concave optimization problem with the iterative calculation by the sequential linearization method using Concave-Convex Procedure. The peak filter which satisfies the robust stability conditions for the MIMO system is designed in the translation along the x axis, automatically, and the reduction of the error in the translation along the x axis is confirmed by the simulation.

The problems of the initial value dependency and the avoidance from the local optimum in Concave-Convex Procedure, selection of the number of the peak filter, tuning the resonant frequency ω of the peak filter, overall optimization including other controllers are future research.

REFERENCES

Araki, M. and Nwokah, O. (1975). Bounds for closed-loop transfer functions of multivariable systems. *IEEE Transactions on Automatic Control*, 20(5), 666–670.

Atsumi, T. and Messner, W.C. (2012). Optimization of Head-Positioning Control in a Hard Disk Drive Using the RBode Plot. *IEEE Transactions on Industrial Electronics*, 59(1), 521–529.

Atsumi, T., Okuyama, A., and Kobayashi, M. (2007). Track-following Control Using Resonant Filter in Hard Disk Drives. In *2007 American Control Conference*, 61–67. IEEE.

Butler, H. (2011). Position Control in Lithographic Equipment [Applications of Control]. *IEEE Control Systems*, 31(5), 28–47.

Do, T.M.T. and Artieres, T. (2012). Regularized bundle methods for convex and non-convex risks. *Journal of Machine Learning Research*, 13, 3539–3583.

Gaing, Z.L. (2004). A Particle Swarm Optimization Approach for Optimum Design of PID Controller in AVR System. *IEEE Transactions on Energy Conversion*, 19(2), 384–391.

Hast, M., Astrom, K., Bernhardsson, B., and Boyd, S. (2013). PID design by convex-concave optimization. In *2013 European Control Conference (ECC)*, 4460–4465. IEEE.

Karimi, A. and Galdos, G. (2010). Fixed-order H_∞ controller design for nonparametric models by convex optimization. *Automatica*, 46(8), 1388–1394.

Kitayoshi, R. and Fujimoto, H. (2019). Automatic adjustment method of controller structure and parameter based on Structured H_∞ control. In *IECON 2019 - 45th Annual Conference of the IEEE Industrial Electronics Society*, 3111–3116.

Lee, S., Marsolan, N., Sun, T., Lee, S., and Kilian, B. (1985). Application of Self-Optimizing Controllers to Variable Time-Delay Processes. In *Proceedings of the 1985 American Control Conference*, 1275–1280.

Lofberg, J. (2004). YALMIP : a toolbox for modeling and optimization in MATLAB. In *2004 IEEE International Conference on Robotics and Automation (IEEE Cat. No.04CH37508)*, 284–289. IEEE.

Mae, M., Ohnishi, W., Fujimoto, H., and Hori, Y. (2019). Perfect Tracking Control Considering Generalized Controllability Indices and Application for High-Precision Stage in Translation and Pitching. *IEEJ Journal of Industry Applications*, 8(2), 263–270.

Maeda, Y. and Iwasaki, M. (2014). Circle Condition-Based Feedback Controller Design for Fast and Precise Positioning. *IEEE Transactions on Industrial Electronics*, 61(2), 1113–1122.

MosekApS (2019). MOSEK Optimization Toolbox for MATLAB 9.0.88.

Nakamura, K., Yubai, K., Yashiro, D., and Komada, S. (2017). Fully Parameterized Controller Design Method for High Control Bandwidth Using Frequency Response Data Sets. In *The 3rd IEEJ international workshop on Sensing, Actuation, Motion Control, and Optimization (SAMCON 2017)*.

Ohnishi, W. (2019). Data-based feedback controller tuning utilizing collocated and non-collocated sensors. In *Joint 8th IFAC Symposium on Mechatronic Systems and 11th IFAC Symposium on Nonlinear Control Systems*.

Oomen, T. (2018). Advanced Motion Control for Precision Mechatronics: Control, Identification, and Learning of Complex Systems. *IEEJ Journal of Industry Applications*, 7(2), 127–140.

Rosenbrock, H. (1969). Design of multivariable control systems using the inverse Nyquist array. *Proceedings of the Institution of Electrical Engineers*, 116(11), 1929.

Sebe, N. (1996). Diagonal dominance and integrity. In *Proceedings of 35th IEEE Conference on Decision and Control*, volume 2, 1904–1909. IEEE.

Shinoda, S., Yubai, K., Yashiro, D., and Hirai, J. (2017). Multivariable Controller Design Achieving Diagonal Dominance Using Frequency Response Data. *Electronics and Communications in Japan*, 100(10), 12–23.

Tang, K., Kim Fung Man, Guanrong Chen, and Kwong, S. (2001). An optimal fuzzy PID controller. *IEEE Transactions on Industrial Electronics*, 48(4), 757–765.

Yuille, A.L. and Rangarajan, A. (2003). The Concave-Convex Procedure. *Neural Computation*, 15(4), 915–936.